European Review for Medical and Pharmacological Sciences 2017; 21: 4989-4998

Rapamycin facilitates fracture healing through inducing cell autophagy and suppressing cell apoptosis in bone tissues

Z.-Y. YIN[1], J. YIN[2], Y.-F. HUO[1], J. YU[1], L.-X. SHENG[1], Y.-F. DONG[1]

[1]Department of Orthopedics, the Affiliated Lianyungang Hospital of Xuzhou Medical University, The First People's Hospital of Lianyungang, Lianyungang, China
[2]Department of Orthopedics, the Affiliated Jiangning Hospital of Nanjing Medical University, Nanjing, China

Zhaoyang Yin and *Jian Yin* contributed equally to this work

Abstract. – OBJECTIVE: To investigate the changes in cell autophagy and the molecular mechanism of rapamycin affecting the fracture healing.

MATERIAL AND METHODS: Sprague-Dawley (SD) rats were used to establish the right femoral shaft fracture models, and then underwent immunofluorescence assay to detect the autophagy level in bone tissues. After model establishment, SD rats were divided into two groups, the control group and the rapamycin group (1 mg/kg/d). Respectively, at the 2nd, 4th, and 6th week, rats were randomly selected from each group for X-ray and Micro-computed tomography (Micro-CT) examinations to determine callus growth, immunofluorescence assay to detect the protein expression of light chain 3 II (LC3 II), immunohistochemistry to evaluate the autophagy level through detecting the expression of Beclin1 in rats, Western blotting assay to detect cell apoptosis in tissues, hematoxylin and eosin staining (HE staining) to evaluate the osteoblastic activity through count of osteoblast in bone tissue at the end of fracture, and measure the expression of vascular endothelial growth factors (VEGF).

RESULTS: Significant increases were seen in protein expression of cells in bone tissues at the end of fracture. In rapamycin group, callus formation and calcification level in rats were all higher than those in control group; compared with control group, for rats in rapamycin group, cell autophagy was significantly elevated in bone tissues, while cell apoptosis at the end of fracture was reduced with a significant increase in osteoblastic activity. The expression of VEGF in rapamycin group was higher than that in control group.

CONCLUSIONS: Rapamycin can facilitate fracture healing through inducing cell apoptosis and suppressing cell apoptosis in bone tissues.

Key Words:
Fracture healing, Apoptosis, Autophagy, Rapamycin.

Introduction

Fracture healing is a complicated but orderly process regulated by a variety of histological changes and biochemical changes. During the whole process of fracture healing, cells of bone tissues surrounding the fracture end, activity of immunological cells, blood supply in bone tissues after fracture and regulatory effect of cytokines, are also of great significance[1]. Currently, a great number of literature reported studies on molecular signal pathway, expression of major proteins and regulation of cytokines in fracture healing[2]. Nevertheless, in spite of the sufficient understanding on morphological research of fracture healing, specific cell molecular mechanism about fracture healing remains unclear yet. Scholars believe that fracture healing is caused by a series of process dominated by cells; thus, cellular mechanism has been regarded as the major mechanism of fracture healing[3].

Cell autophagy refers to a process, in which intracellular macromolecules or dysfunctional organelles are degraded into the substances nourishing the cells, or those that can be re-used for assembling the new organelles[4]. Latest research has shown that under stress environment like disease or trauma, the activity of cells is sustained through activating and initiating the autophagy mechanism in cells, thereby surviving in the adverse environment, like disease and trauma[5]. In addition, studies have also confirmed the outstanding roles of cell

Corresponding Author: Yuefu Dong, MD; e-mail: dongyuefu@163.com

autophagy in cancer, myocardial infarction, hypertension, diabetes mellitus and neurological disorder, based on which they also put forward available strategies for treatment of corresponding diseases through regulating the autophagic level of cells[6-8]. In a study, researchers conducted a series of measurements using immune markers to compare the quantity of light-chain 3 (LC3, the marker protein of autophagosome) of bone cells and osteoblasts in tibia of mice, and the results showed that autophagy level in bone cells was higher than that in the osteoblasts[9]. In the hypoxia environment with insufficient nutrition, the activity of bone cells is sustained through initiating cell autophagy. However, for cells in bone tissues at fracture end, cell autophagy is vital to the maintenance of survival of bone cells[10].

In the signal transduction pathway of cell autophagy, mammalian target of rapamycin (mTOR) is a key link in regulation of pathway activity[11]. mTOR, a core part connecting with various intracellular signal pathways, significantly affects the growth, differentiation and proliferation of cells. In addition, mTOR acts as the upstream regulatory protein in autophagic pathway. Rapamycin can increase the autophagic level of cells through inhibiting the activity of mTOR[12].

Material and Methods

Animals and Reagents

Clean, adult, male, Sprague-Dawley rats aged above 3 months with weight between 230-270 g were selected for this study. All rats were in normal nutrition and mental condition and were provided by Qinglongshan Experimental Animal Center (Nanjing, Jiangsu, China). This study was approved by the Animal Ethics Committee of Xuzhou Medical University Animal Center. Beclin1 and LC3II antibodies were purchased from Sigma-Aldrich (St. Louis, MO, USA), TdT-mediated dUTP nick end labeling (TUNEL) kit and ALP kit for activity detection were purchased from Beyotime (Shanghai, China), and vascular endothelial growth factor (VEGF), mTOR and p-mTOR antibodies were purchased from CST (Danvers, MA, USA).

Model Establishment and Grouping

Rats were randomly divided into two groups, and after one week of feeding, models were prepared in accordance with the methods proposed by Holstein et al[13]. After anesthesia, a transverse incision in length of about 3 cm was prepared on lateral part of right femoral shaft to expose the right femoral shaft that was later cut transversely. Thereafter, along the inner edge in *patella* of right lower limb, a vertical incision in length of about 1 cm was made, through which tissues of quadriceps tendon were cut to expose the intercondylar *fossa* femur. After marrow was enlarged, a Kirschner's wire in diameter of 1.0 mm was reversely inserted under direct view to enclose the fracture end, and X-ray examination (Siemens, Berlin, Germany) was performed and recorded after suture of incision.

In experiment of autophagy detection at fracture end, rats were divided into the blank control group and groups of different time points of model-establishment (12 h, 24 h, day 3, and 7). For assessing the effect of rapamycin, rats were divided into control group and rapamycin group (intraperitoneal injection of 1 mg/kg).

Immunofluorescence Assay

Paraffin-embedded callus tissues were sequentially sliced into sections of 4 μm and heated at 60°C overnight. Following dewaxing using xylene and dehydration using ethanol of gradient concentrations, antigen retrieval and blocking with serum were performed. Thereafter, LC3 II antibody was added into the sections for incubation at 4°C overnight. Next day, sections were rinsed followed by the addition of secondary antibody, and then placed under the fluorescent microscope for observation after being sealed using the anti-cancellation mounting medium containing DAPI (4,6-diamidino-2-phenylindole).

Hematoxylin and Eosin (HE) Staining

Paraffin-embedded callus tissues were sequentially sliced into sections of 4 μm and heated at 60°C overnight. Following dewaxing using xylene (Biosharp, Hefei, China) and dehydration using ethanol of gradient concentrations, sections were stained with hematoxylin and eosin followed by examination of 3 planes of each sample using Image-Pro Plus IPP (Mediaplayer, NY, USA). The number of osteoblast in each section was measured.

Immunohistochemistry Staining of Beclin1

Paraffin-embedded callus tissues were sequentially sliced into sections followed by dewaxing using xylene and dehydration using ethanol of gradient concentrations. Sections were incubat-

ed in warm deionized water containing 0.3% H_2O_2 (Guge Biotech, Nanjing, China) for 30 min, blocked using serum with the endogenous peroxide being eliminated, and incubated with primary antibody at 4°C overnight. In following day, horseradish peroxidase-labeled immunoglobulin G (IgG) was added for incubation, and sections were then transferred into the mixtures prepared using the ABC kit (Albumin and biotin). After 10 min of DAB (3,3'-diaminobenzidine) reaction for color development, sections were re-dyed with hematoxylin, rinsed, dehydrated and cleaned followed by observation under microscope.

Qualitative Aanalysis of X-ray Examination of Callus

After operation, SD rats in each group received the anterior and posterior X-ray examinations at the 2nd, 4th, and 6th weeks in same settings (supine position with a 90° angle in right femoral shaft through coxa and knee bending. Exposure settings: 45 kV, 1 kV, intercept of 0.08 s and 70 mA). With Garrett Scoring System as an indicator of fracture healing, we evaluated the fracture healing based on the image data of X-ray examination.

Quantitative analysis of micro-CT Examination of Callus

After photographing, fracture samples were collected from SD rats that were executed using anhydrous ether with callus being retained and Kirschner's wire being removed, and fixed in 10% neutral formaldehyde. After 24 to 48 h, micro-CT was sequentially performed for those samples (micro CT40; ScaInco Medical, Bassers-dorf, Switzerland). Scanning procedure was initiated from a region in length of 10 mm at fracture along the long axis of femoral shaft, and all sectional pictures were analyzed to calculate the area of bone trabecula (BA), area of sample (SA) and mean trabecula plate density (MTPD).

Western Blotting

Callus tissues that were extracted from SD rats were ground in liquid nitrogen, diluted in normal saline and placed on ice for collecting the supernatant followed by centrifugation at 4°C for 5 min with the supernatant being discarded. Sediment was resuspended using radio-immunoprecipitation assay (RIPA) lysis buffer containing phenylmethanesulfonyl fluoride (PMSF), and the lysate was centrifuged at 16000 g and 4°C for 15 min. Supernatant was taken for protein quantification, and proteins were added into the loading buffer for denaturation by heating. Denatured proteins were loaded for sodium dodecyl sulfate polyacrylamide gel electrophoresis (SDS-PAGE) followed by member-transfer, in which membrane was blocked using 5% skimmed milk for 2 h. Primary antibody was added to the membrane for incubation overnight at 4°C; after washing for 3 times using Tris-buffer saline + Tween 20 (TBST), 10 min for each time, corresponding secondary antibody was added to the membrane for incubation at room temperature for 1 h followed by TBST washing for 3 times, 10 min for each time, and enhanced chemiluminescence (ECL) was adopted for detecting the protein expressions in different samples.

Statistical Analysis

Data were presented as mean ± standard deviation, and analyzed in Statistical Product and Service Solutions 13.0 (SPSS Inc., Chicago, IL, USA). In this study, one-way analysis of variance followed by Least Significance as the Post-Hoc Test was performed, and $p < 0.05$ suggested that the difference had statistical significance.

Results

Autophagy Level is Increased in Fracture Healing

Autophagy level in tissues was detected *via* LC3 II immunofluorescence assay, and results showed the LC3 II expressions in normal bone tissues and fracture bone tissues. At different time points after fracture, tremendous protein expression of LC3 II was identified, and the positive rates of LC3-II at different time points were all higher than those in the blank control group ($p < 0.05$; Figure 1A). Within 24 h after model establishment, the positive rate of LC3 II reached highest (92.34 ± 2.67) % followed by a gradual decrease, and at day 3 and 7, the positive rates were respectively (85.77 ± 3.7) % and (67.44 ± 2.89) %, still higher than those in the blank control group ($p < 0.05$; Figure 1B).

Rapamycin Facilitates the Fracture Healing

X-ray examination was performed for detecting the callus formation. At the 2nd week after establishment of fracture model, the results of X-ray examination showed that Kirschner's wires were all positioned as predicted and fracture

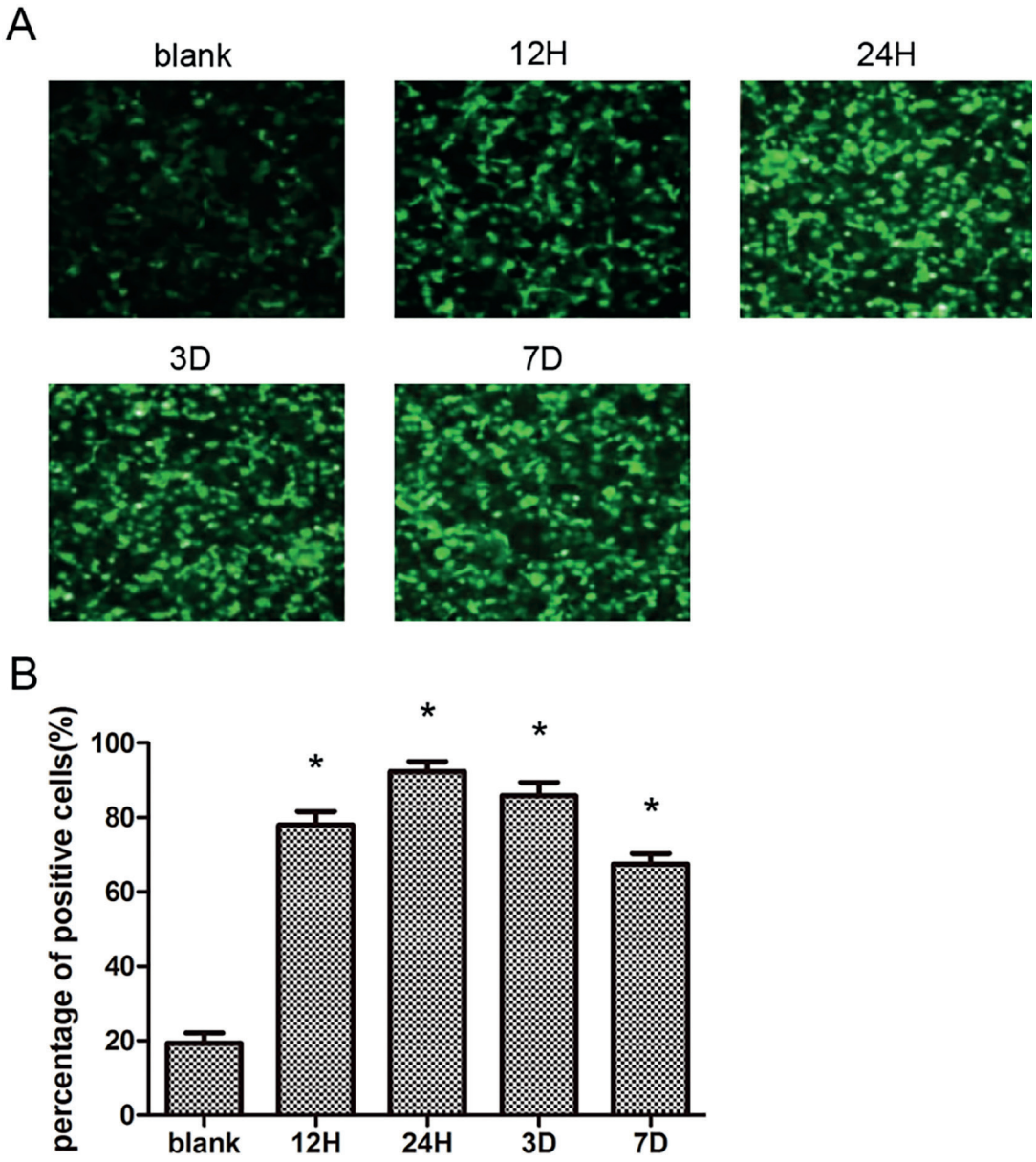

Figure 1. Immunofluorescent assay of LC3 II in callus tissues during fracture healing. ***(A)*** Immunofluorescent assays of LC3 II in callus tissues in blank control group and respectively at 12 h, 24 h, 3 d and 7 d after fracture (200×); ***(B)*** Cell count of LC-II positive cells. *Compared with the blank control group, $p < 0.05$.

end was in good alignment. In control group, surrounding the fracture line that was relatively clear, there was a little discontinuous and cloudy callus formation; in rapamycin group, significant callus growth was identified at fracture end of femoral shaft of rat, and fracture line turned obscure. At the 4th week, in control group, continuous callus growth was identified in a small amount, while the fracture line became a little vague. In rapamycin group, the callus at fracture end was significantly thickened compared with the thickness of callus at the 2nd week with an obscure fracture line. At the 6th week, in control group, formation of bone bridge was seen in cortex of bone with the remodeling of callus; while in rapamycin group, fracture line disappeared, and remodeling of callus was initiated (Figure 2A). With Garrett scoring system, quantitative analysis was performed among three groups, and the results showed that compared with the control group, rapamycin could significantly improve the healing quality (Figure 2B; $p < 0.05$).

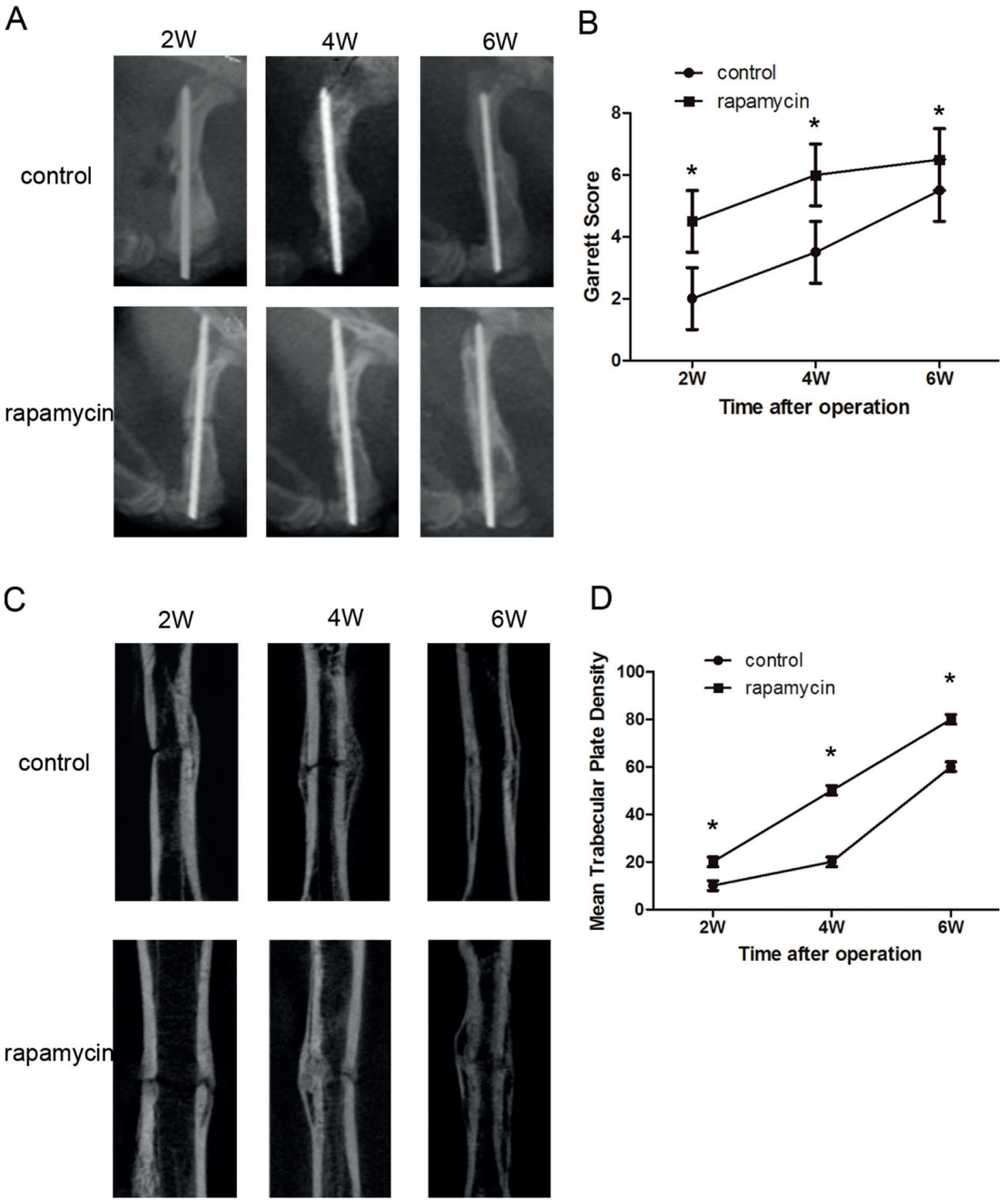

Figure 2. Function assessment in fracture healing. ***(A)*** X-ray examination for detection of healing of femoral shaft fracture at the 2nd, 4th, and 6th weeks in mice of control group and rapamycin group; ***(B)*** Garrett score for X-ray examination of mice at the 2nd, 4th, and 6th weeks in mice of control group and rapamycin group; ***(C)*** Micro-CT examination for detection of healing of femoral shaft fracture at the 2nd, 4th, and 6th weeks in mice of control group and rapamycin group; ***(D)*** Score of bone density in mice at the 2nd, 4th, and 6th weeks in mice of control group and rapamycin group. *Compared with the control group at the same time poin, $p < 0.05$.

Callus formation was detected through micro-CT examination. At the 2nd week after establishment of fracture model in SD rats, callus formation was identified at fracture end, but fracture part was less enclosed by callus; in rapamycin group, mass callus generation was seen at fracture end of femoral shaft in rats. At the 4th week, in control group, callus formation was remarkably increased when compared with the formation before operation, and callus was most-

ly distributed around the majority of bone tissues. Also, fracture end was filled by some newly generated bone tissues. In rapamycin group, fracture end of femoral shaft of rats was filled by a great amount of newly generated bone mass with an increase in thickness of callus. At the 6th week, fracture end was completely filled by regenerated bone tissues and fused with the cortex; while in rapamycin group, callus remodeling was initiated with an increased calcification (Figure 2C and 2D; $p < 0.05$).

Rapamycin Suppresses Cell Apoptosis at Fracture End

HE staining was utilized to observe histological changes in fracture healing. At the 2nd week after model establishment, bone trabeculae in control group were sparsely distributed with a widened trabecular space, where growth of chondrocytes could be identified; while in rapamycin group, bone trabeculae were interlaced and in well alignment. At the 4th week, continuous growth of bone trabeculae was seen with a reduction in trabecular space and increases in quantities of osteoblasts surrounding the bone trabecula in each group. At the 6th week, the quantity of bone trabeculae was increased in comparison with that at the 4th week, and fusion between trabeculae was occasionally seen, but there were still bone trabeculae with a larger width; in rapamycin group, bone trabeculae were fused markedly with formation of woven bones (Figure 3A).

Western blotting assay was performed to detect cell apoptosis in fracture healing of bones, and the results suggested that the content of apoptotic proteins in both groups was decreased with extension of time; at different time points, we also compared the protein expression between two groups, and found that in rapamycin group, the expressions of Bax (Bcl-2 Associated X Protein) were all significantly lower than those in the control group ($p < 0.05$), while the Bcl-2 (B-cell lymphoma-2) was upregulated in comparison with the control group ($p < 0.05$). Results of gray scale scanning and statistics showed that ratios of Bcl-2 to Bax in rapamycin group were all higher than those in the control group ($p < 0.05$; Figure 3B, 3D and 3E).

Western blotting assay was also performed for detecting the level of VEGF in callus tissues, and the results showed that at different time points after model establishment, the activity of VEGF in control group was lower than that in the rapamycin group ($p < 0.05$; Figure 3B and 3C).

Rapamycin Increases the Cell Autophagy in Fracture Tissues

In two groups, we measured the expressions of Beclin1 and LC3 II. The fluorescent detection of LC3 II showed that proteins were expressed in cytoplasm and spread sporadically. At different time points, the protein expression of LC3 II in control group was significantly lower than that in rapamycin group and the difference had statistical significance ($p < 0.05$; Figure 4A and 4B). The results showed that Beclin1 protein was mainly distributed in cellular membrane and cytoplasm (Figure 4C), and statistics on positive rates of proteins at different time points showed that compared with the control group, the level of proteins was significantly higher in rapamycin group ($p < 0.05$; Figure 4D).

Rapamycin Suppresses mTOR Pathway

Additionally, Western blotting assay was carried out to measure the levels of mTOR and p-mTOR in callus, and results showed that at different time points after model establishment, the activity of p-mTOR in control group was significantly lower than that in rapamycin group ($p < 0.05$); besides, p-mTOR/mTOR ratios at different time points after model establishment in control group were all lower than those in rapamycin group ($p < 0.05$; Figure 5A, 5B and 5C).

Discussion

Autophagy mechanism is highly conservative in evolution and exists widely in eukaryotic cells. In recent years, people are increasingly interested in autophagy, and have found that autophagy mechanism is of great significance in courses of pains, cardiovascular and endocrine diseases. Regulation of autophagy is mediated by autophagy associated genes (ATG), wherein Beclin1 and LC3 are important ATGs in autophagy[14]. In response to the adverse condition, cells can initiate the autophagic function for survival[15], based on which we supposed that autophagic levels in cells of bone tissues around the trauma will be correspondingly changed. Through model establishment and Western blotting assay of LC3 protein expression, we found that the autophagic level in cells of fracture tissues was significantly elevated followed by a slight decrease after 24 h, but remaining higher than the level in nor-

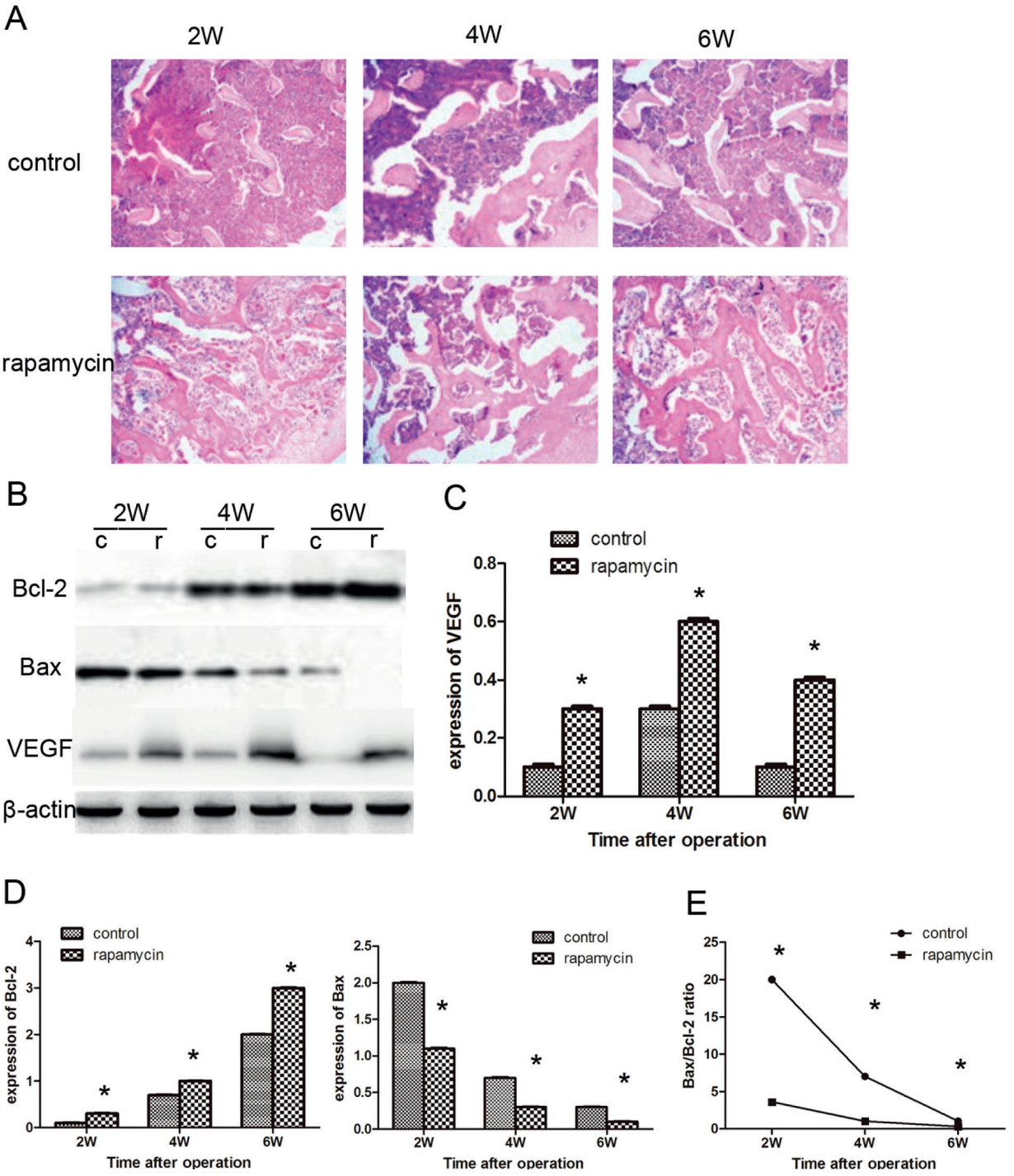

Figure 3. Detection of histological changes in fracture healing. ***(A)*** HE staining for evaluating healing of femoral shaft fracture at the 2nd, 4th, and 6th weeks in mice of control group and rapamycin group (400×); ***(B)*** Western blotting assay for evaluating the expression levels of Bax, Bcl-2 and VEGF at the 2nd, 4th, and 6th weeks in mice of control group and rapamycin group; ***(C)*** Gray scale scanning of protein expression of VEGF; ***(D)*** Gray scale scanning of protein expression of Bax, Bcl-2 and VEGF; ***(E)*** Data analysis of Bax/Bcl-2 ratio. *Compared with the control group at the same time point, $p < 0.05$.

mal bone tissues, suggesting that cell autophagy during fracture healing is activated and sustains at a higher level.

In fracture healing, the osteoblasts are originated from the mesenchymal stem cells, and then differentiated into the mature osteoblasts[16].

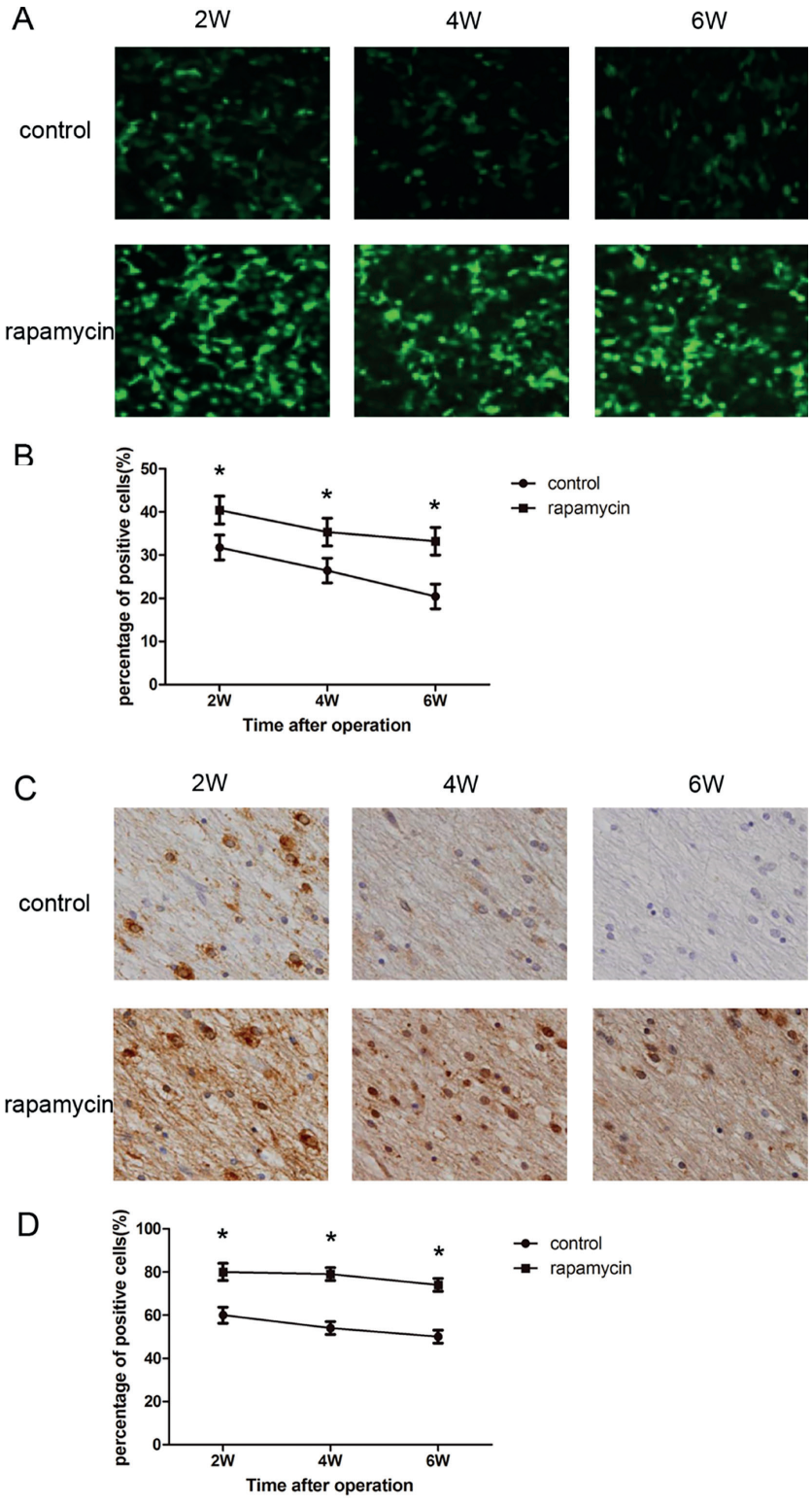

Figure 4. Detecting the effect of rapamycin on autophagy in fracture healing. ***(A)*** Immunofluorescent assay for evaluating autophagy level in femoral shaft at the 2nd, 4th, and 6th weeks in mice of control group and rapamycin group; ***(B)*** Statistics on ratios of positive cells in immunofluorescent assay of LC3 II at the 2nd, 4th, and 6th weeks in mice of control group and rapamycin group; ***(C)*** Immunohistochemistry staining of Beclin1 for evaluating autophagy level in femoral shaft at the 2nd, 4th, and 6th weeks in mice of control group and rapamycin group; ***(D)*** Statistics on ratios of positive cells in immunofluorescent assay of Beclin1 at the 2nd, 4th, and 6th weeks in mice of control group and rapamycin group. *Compared with the control group at the same time point, $p < 0.05$ (400×).

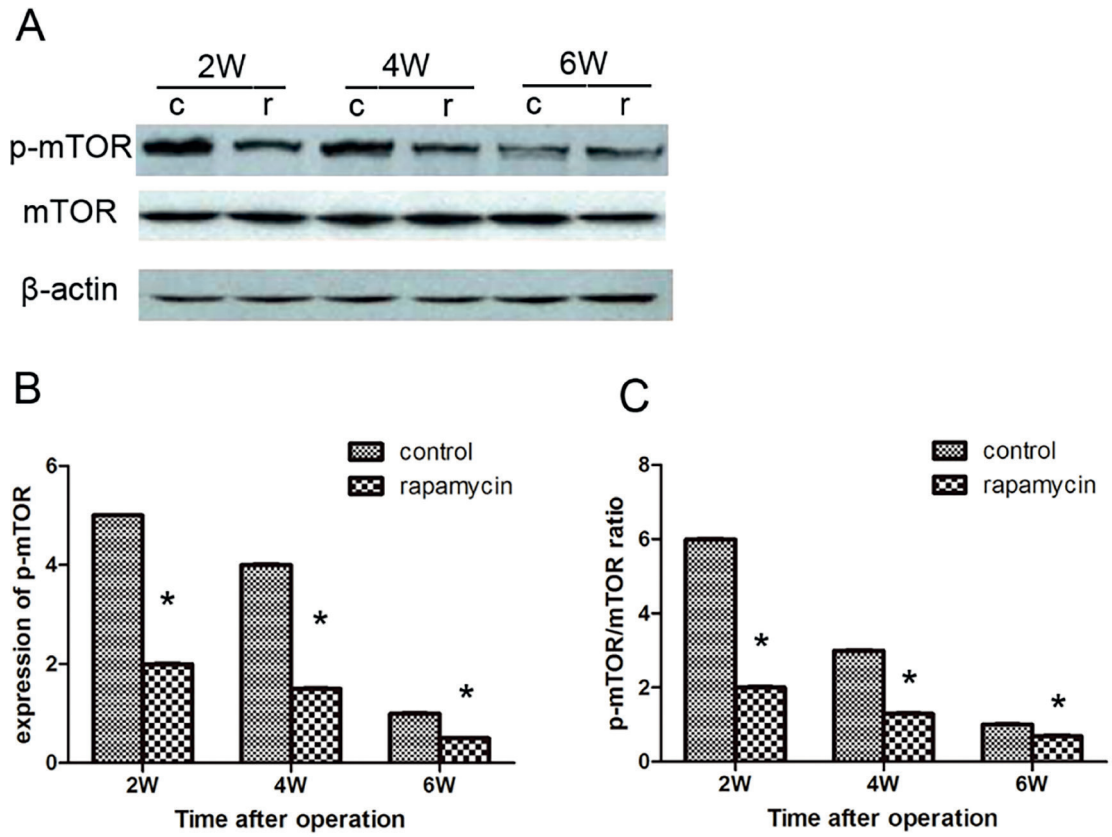

Figure 5. Detection of mTOR pathway via Western blotting assay. ***(A)*** Western blotting assay for assessing the protein expressions of mTOR and p-mTOR in femoral shaft tissues at the 2nd, 4th, and 6th weeks in mice of control group and rapamycin group; ***(B)*** Gray scale scanning of protein expression of p-mTOR; ***(C)*** Statistics on p-mTOR/mTOR ratio. *Compared with the control group at the same time point, $p < 0.05$.

Those mature osteoblasts aggregate on surface of bone, or present as apoptotic cells. Apoptosis is a programmatic cell death, which is a physiological process to eliminate the dysfunctional or damaged cells[17]. During fracture healing, suppressing the apoptosis of osteoblasts is considered as a necessary link to facilitate the aggregation of active osteoblasts. In this study, we found that rapamycin could significantly accelerate the fracture healing, while results of X-ray examination and micro-CT examination further proved the accelerating effect of rapamycin on effective healing of fracture end. Meanwhile, Western blotting assay showed that rapamycin could inhibit cell apoptosis at fracture end, thereby facilitating the expression of VEGF. These results confirmed that rapamycin could inhibit cell apoptosis, regulate the angiogenesis and accelerate the effective fracture of fracture.

mTOR is an upstream regulation protein in autophagy pathway, and with a higher activity, it can suppress the downstream signal protein of autophagy to suppress cell autophagy. Thus, inhibition on protein activity of mTOR by rapamycin can decrease the suppression of mTOR on downstream signal proteins, thereby activating the signal pathway of autophagy and upregulating the autophagy level of cells[18]. In this study, the results indicated that rapamycin could significantly inhibit the mTOR pathway, and increase cell autophagy in tissues at fracture end. We suggested that the positive effect of rapamycin on fracture healing might be generated by inducing cell autophagy and inhibiting cell apoptosis through this pathway.

Conclusions

During fracture healing, cell autophagy at fracture end is significantly elevated, and in *vivo* administration of rapamycin can further increase cell autophagy and downregulate cell apoptosis at fracture end, thereby facilitating the rate and quality of fracture healing.

Conflict of Interest

The Authors declare that they have no conflict of interests.

References

1) Nelson FR, Brighton CT, Ryaby J, Simon BJ, Nielson JH, Lorich DG, Bolander M, Seelig J. Use of physical forces in bone healing. J Am Acad Orthop Surg 2003; 11: 344-354.
2) Crockett JC, Rogers MJ, Coxon FP, Hocking LJ, Helfrich MH. Bone remodelling at a glance. J Cell Sci 2011; 124: 991-998.
3) Martin T, Gooi JH, Sims NA. Molecular mechanisms in coupling of bone formation to resorption. Crit Rev Eukaryot Gene Expr 2009; 19: 73-88.
4) Baudhuin P, Beaufay H, De Duve C. Combined biochemical and morphological study of particulate fractions from rat liver. Analysis of preparations enriched in lysosomes or in particles containing urate oxidase, D-amino acid oxidase, and catalase. J Cell Biol 1965; 26: 219-243.
5) Shen HM, Codogno P. Autophagic cell death: loch ness monster or endangered species? Autophagy 2011; 7: 457-465.
6) Wang ZC, Liu Y, Wang H, Han QK, Lu C. Research on the relationship between artesunate and Raji cell autophagy and apoptosis of Burkitt's lymphoma and its mechanism. Eur Rev Med Pharmacol Sci 2017; 21: 2238-2243.
7) Wang Y, Liu J, Tao Z, Wu P, Cheng W, Du Y, Zhou N, Ge Y, Yang Z. Exogenous HGF prevents cardiomyocytes from apoptosis after hypoxia via up-regulating cell autophagy. Cell Physiol Biochem 2016; 38: 2401-2413.
8) Singh R, Xiang Y, Wang Y, Baikati K, Cuervo AM, Luu YK, Tang Y, Pessin JE, Schwartz GJ, Czaja MJ. Autophagy regulates adipose mass and differentiation in mice. J Clin Invest 2009; 119: 3329-3339.
9) Zahm AM, Bohensky J, Adams CS, Shapiro IM, Srinivas V. Bone cell autophagy is regulated by environmental factors. Cells Tissues Organs 2011; 194: 274-278.
10) Manolagas SC, Parfitt AM. What old means to bone. Trends Endocrinol Metab 2010; 21: 369-374.
11) Kim YC, Guan KL. MTOR: a pharmacologic target for autophagy regulation. J Clin Invest 2015; 125: 25-32.
12) Wu L, Feng Z, Cui S, Hou K, Tang L, Zhou J, Cai G, Xie Y, Hong Q, Fu B, Chen X. Rapamycin upregulates autophagy by inhibiting the mTOR-ULK1 pathway, resulting in reduced podocyte injury. PLoS One 2013; 8: e63799.
13) Holstein JH, Menger MD, Culemann U, Meier C, Pohlemann T. Development of a locking femur nail for mice. J Biomech 2007; 40: 215-219.
14) Moscat J, Diaz-Meco MT. P62 at the crossroads of autophagy, apoptosis, and cancer. Cell 2009; 137: 1001-1004.
15) Fujita E, Kouroku Y, Isoai A, Kumagai H, Misutani A, Matsuda C, Hayashi YK, Momoi T. Two endoplasmic reticulum-associated degradation (ERAD) systems for the novel variant of the mutant dysferlin: ubiquitin/proteasome ERAD(I) and autophagy/lysosome ERAD(II). Hum Mol Genet 2007; 16: 618-629.
16) Raisz LG. Physiology and pathophysiology of bone remodeling. Clin Chem 1999; 45: 1353-1358.
17) Ghayor C, Rey A, Caverzasio J. Prostaglandin-dependent activation of ERK mediates cell proliferation induced by transforming growth factor beta in mouse osteoblastic cells. Bone 2005; 36: 93-100.
18) Edinger AL, Thompson CB. Defective autophagy leads to cancer. Cancer Cell 2003; 4: 422-424.